frontiers in Marine Science

ORIGINAL RESEARCH
published: 12 December 2017
doi: 10.3389/fmars.2017.00399

Sporochartines A–E, A New Family of Natural Products from the Marine Fungus *Hypoxylon monticulosum* Isolated from a *Sphaerocladina* Sponge

Charlotte Leman-Loubière[1], *Géraldine Le Goff*[1], *Cécile Debitus*[2] *and Jamal Ouazzani*[1]*

[1] Centre National de la Recherche Scientifique, Institut de Chimie des Substances Naturelles ICSN, Gif-sur-Yvette, France, [2] LEMAR, IRD, Centre National de la Recherche Scientifique, IFREMER, Université de Bretagne Occidentale, IUEM, Technopole Brest-Iroise, Plouzané, France

Four new sporochartines B–E were isolated from the marine fungus *Hypoxylon monticulosum* CLL-205, isolated from a sponge belonging to the *Sphaerocladina* order and collected in Tahiti coast. Sporochartine A (**1**), the first representative of this family was previously isolated from the same fungus. The structures of sporochartines B–E were elucidated using 1D and 2D NMR, HRMS and IR data. Their configurations were established according to **ROE correlations and comparison with** the absolute configuration of sporochartine A (**1**) previously obtained from X-ray analysis. Sporochartines A–D (**2–4**) may be derived from endo Diels-Alderase type catalysis and sporochartine E (**5**) from an exo Diels-Alderase catalysis. The spatial conformation of sporochartines drastically influences the results of the cytotoxic bioassay against HCT-116, PC-3, and MCF-7 human cancer cell lines.

Keywords: *Hypoxylon*, *Sphaerocladina*, sporothriolide, sporochartines, cytotoxic compounds

OPEN ACCESS

Edited by:
Antonio Trincone, Istituto di Chimica Biomolecolare (CNR), Italy

Reviewed by:
Johannes F. Imhoff, GEOMAR Helmholtz Centre for Ocean Research Kiel (HZ), Germany
Usama Ramadan Abdelmohsen, University of Würzburg, Germany

***Correspondence:**
Jamal Ouazzani
jamal.ouazzani@cnrs.fr

Specialty section:
This article was submitted to Marine Biotechnology, a section of the journal Frontiers in Marine Science

Received: *17 October 2017*
Accepted: *24 November 2017*
Published: *12 December 2017*

Citation:
Leman-Loubière C, Le Goff G, Debitus C and Ouazzani J (2017) Sporochartines A–E, A New Family of Natural Products from the Marine Fungus Hypoxylon monticulosum Isolated from a Sphaerocladina Sponge. Front. Mar. Sci. 4:399. doi: 10.3389/fmars.2017.00399

INTRODUCTION

The fungal Xylariaceae family includes more than 16 genera and 130 species (Sánchez-Ballesteros et al., 2000) and has been extensively investigated for the chemo diversity and biological activity of their metabolites (Stadler et al., 2006, 2008). Among the 16 genera reported, *Hypoxylon* with 14 species is largely distributed in various marine and terrestrial habitats, and producing a large variety of bioactive compounds among which cohaerins (Quang et al., 2005a; Surup et al., 2013), daldinins and daldinones (Quang et al., 2004; Gu et al., 2007), cytochalasin (Espada et al., 1997), fragiformin (Stadler et al., 2006), mitorubrinols (Quang et al., 2005b), hypoxylonols (Fukai et al., 2012), hypoxylans (Kuhnert et al., 2015a), hypoxyvermelhotins (Kuhnert et al., 2014), rickenyls (Kuhnert et al., 2015b), rutilins (Quang et al., 2005b), carneic acids (Quang et al., 2006), hymatoxins (Bodo et al., 1987; Borgschulte et al., 1991), malettinins (Angawi et al., 2005), hypoxysordarin (Daferner et al., 1999), lenormandins (Kuhnert et al., 2015c), nodulisporic acids (Bills et al., 2012), schweinitzin A (Linh et al., 2014), truncatones (Sudarman et al., 2016), macrocyclic polyesters 15G256 family (Schlingmann et al., 2002), and sporothriolide (Krohn et al., 1994; Surup et al., 2014; Cao et al., 2016).

Sporothriolide belongs to the furofurandione family of natural compounds first published in 1994 (Krohn et al., 1994). This compound exhibits antifungal activity and benefits from substantial

synthetic efforts (Sharma and Krishnnudu, 1995; Yu et al., 2001; Fernandes and Ingle, 2009; Ishihara et al., 2014). The name sporothriolide is related to *Sporothrix* sp. Hektoen and Perkins (strain 700), from which this compound was first isolated. *Sporothrix* genus belongs to a different ascomycete family, ophiostomataceae. The first report on sporothriolide in 1994 detailed both the structure and bioactivity of this product (Krohn et al., 1994). It shows that *Sporothrix* produces sporothriolide, dihydrosporothriolide, as well as various sporothriolide analogs with different side-chain length (canadensolide, discosiolide, avenaciolide, ethiosolide). The authors reported also the antifungal/herbicidal activities of these compounds (Krohn et al., 1994) (**Figure 1**).

Twenty years later, sporothriolide and dihydrosporothriolide were isolated from *Hypoxylon monticulosum* together with three monocyclic acid precursors: sporothric acid, isosporothric acid and dihydroisosporothric acid (**Figure 1**) (Surup et al., 2014). More recently, sporothriolide was isolated from *Nodulisporium* sp., an anamorph of *Hypoxylon*, and the herbicidal activity was confirmed (Cao et al., 2016).

In our previous contribution, we added to the scarce sporothriolide family two new compounds, deoxysporothric acid and a new complex architecture sporochartine A, combining sporothriolide and trienylfuranol A moieties. The trienylfuranol A was recently isolated from a different *Hypoxylon submoniticulosum* (Burgess et al., 2017).

In the present work we report four new sporochartines B to E. Their structures were elucidated using 1D and 2D NMR, HRMS, IR and comparison with sporochartine A data, for which the absolute configuration was previously established by X-Ray analysis. A Diels-Alderase type reaction is probably involved in the biosynthesis of the five isolated sporochartines, as discussed below.

The human cancer cell-lines cytotoxicity bioassay shows that the conformation of sporochartines has an impact on the biological activity.

RESULTS AND DISCUSSION

According to our previous work, sporochartine A (**1**) was obtained after 5 days cultivation of *H. monticulosum* CLL-205 in PDB broth (Leman-Loubière et al., 2017). By extending the cultivation of the same microorganism by a further 4 days, the

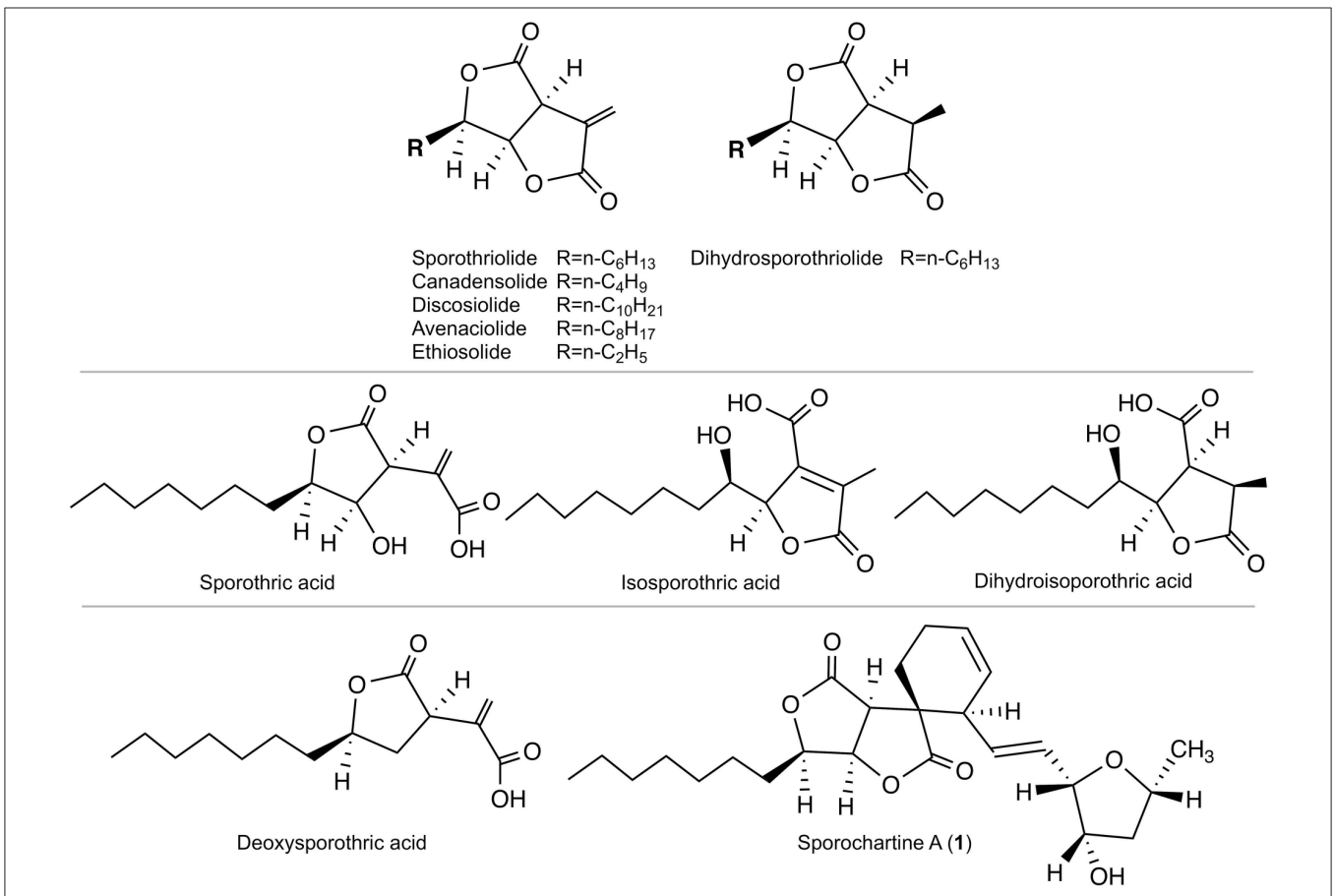

FIGURE 1 | Top: Sporothriolide and analogs reported in 1994 (Krohn et al., 1994). **Middle:** Monocyclic precursors reported in 2014 (Surup et al., 2014). **Bottom:** Deoxysporothric acid and sporochartine A reported in our previous work (Leman-Loubière et al., 2017).

ethyl actetate extract gives the HPLC chromatogram presented in **Figure 2**.

Sporochartines B–D were isolated as white powders by flash chromatography followed by semi-preparative HPLC. They had similar $[M+H]^+$ HRESIMS molecular weights, molecular formula $C_{24}H_{34}O_6$ and IR spectra compared with sporochartine A (**1**) (**Table 2**) (Leman-Loubière et al., 2017). The ^1H and ^{13}C NMR spectra of sporochartines B–D were similar to those of compound **1** (**Tables 1**, **2**). Optical rotations $[\alpha]_{25}^{D}$, IR bands and HRESIMS are reported in **Table 2**.

COSY and HMBC spectra, confirmed that sporochartines A–D had the same connectivities supporting similar planar scaffold (**Figure 3**). In addition, the common coupling constant of 15.4–15.6 Hz between H-18 and H-19 confirmed that the double bond C-18/C-19 is in *E* configuration.

Based on the previously reported absolute configuration of sporochartine A (**1**) and ROE correlations, we deduced the absolute configuration of sporochartines B–D (**2–4**) (**Figure 4**).

The common ROE correlations between H-2 and H-5 and between H-5 and H-6 requiring a *cis* orientation of these three protons was found in the sporochartine A–D. Therefore, the stereochemistry of the sporothriolide moiety was identical. Moreover, based on ROE correlations between H-20 and H-21 and between H-21 and H-23, the strerochemistry of the tetrahydrofurane moiety is also a common feature in sporochartines A–D.

For sporochartine B (**2**) (**Figure 4**), we did not observe ROE correlations between H-17 and H-2 and between H-17 and H-14b as in sporochartine A (**1**), while a new correlation is observed between H-17 and H-13. This data suggests that the carbon C-17 have opposite stereochemistry compared to **1** supporting a *3S,17R* configuration of **2** (instead of *3S,17S* in **1**).

For sporochartine C (**3**) (**Figure 4**), the H-17/H-2 and H-17/H-14b correlations observed in sporochartine A (**1**) are absent. In addition, we observed a correlation between H-17 and H-13 and H-2 and H-14a in compound **3**. Based on this data, we suggest that compound **3** has a *3R,17S* configuration.

Sporochartine D (**4**) (**Figure 4**) conserved the correlations between H-17 and H-2 and between H-17 and H-14b reported for sporochartine A (**1**). Furthermore, the correlation between H-17 and H-13 is absent in both **4** and **1**. In **4** we have an additional correlation between H-13 and H-2, absent in **1**. These observations support the conclusion that **4** is the *3R,17R* isomer of **1**.

A new compound referred as sporochartine E (**5**) was also isolated as a white powder. Compound **5** has the same molecular formula $C_{24}H_{34}O_6$ as compound **1**, deduced from HRESIMS *m/z* $[M+H]^+$ 419.2433. Here again we have eight degrees of unsaturation accounting for two γ-lactones, two double bonds, one six-membered cycle moiety and one tetrahydrofurane moiety.

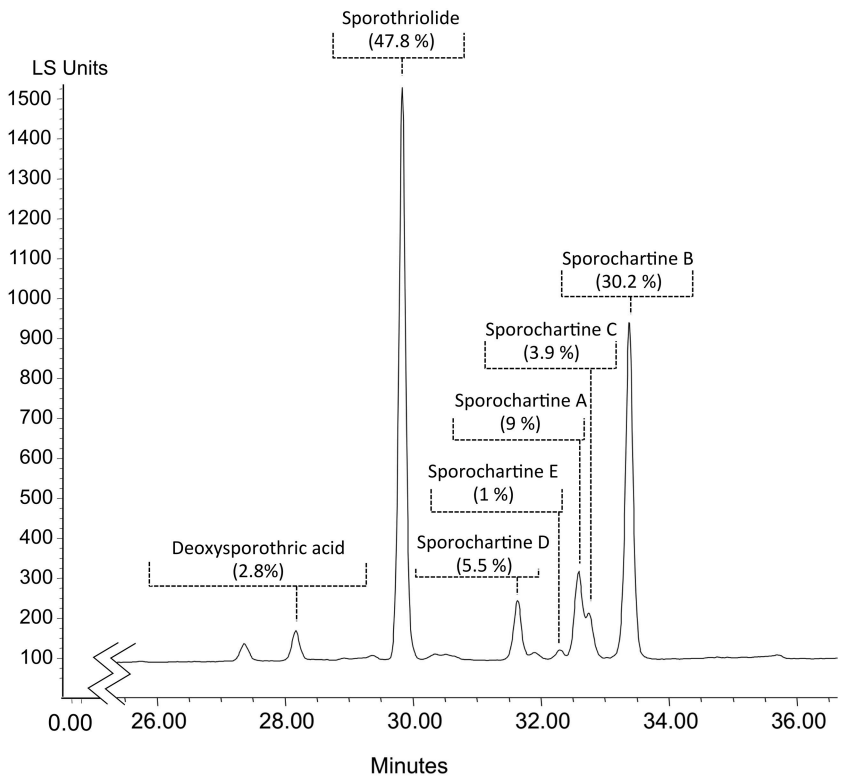

FIGURE 2 | HPLC analysis of the ethyl acetate extract of *Hypoxylon monticulosum* CLL-205 cultivated in PBD for 9 days. Percentages were deduced from peak integration based on Light Scattering Detection chromatogram (LSD).

TABLE 1 | ^{1}H NMR data for sporochartines A–E (Data acquired in $CDCl_3$ at 500 MHz).

Position	Sporochartine A	Sporochartine B	Sporochartine C	Sporochartine D	Sporochartine E
	δ_H mult, (*J* in Hz)	δ_H mult, (*J* in Hz)	δ_H mult, (*J* in Hz)	δ_H mult, (*J* in Hz)	δ_H (*J* in Hz)
2	3.32, d (5.3)	3.30, d (5.8)	3.24, d (5.9)	3.30, d (5.2)	3.42, d (5.9)
5	5.10, dd (3.5, 5.3)	5.13, dd (4.3, 5.9)	5.01, dd (4.2, 5.8)	5.09, dd, (3.6, 5.2)	4.97, dd (4.1, 5.8)
6	4.45, m	4.39, m	4.40, m	4.45, m	4.44, m
7	1.78, m	1.76, m	1.76, m	1.82, m	1.81, m
	1.91, m	1.85, m	1.85, m	1.91, m	1.89, m
8	1.45, m	1.45, m	1.45, m	1.47, m	1.44, m
9	1.37, m	1.34, m	1.34, m	1.37, m	1.36, m
10	1.30, m	1.29, m	1.29, m	1.30, m	1.29, m
11	1.30, m	1.29, m	1.29, m	1.30, m	1.28, m
12	0.89, t (6.8)	0.88, t (6.9)	0.89, t (6.9)	0.89, t (7.0)	0.88, t (6.8)
13	2.00, m	2.04, m	2.02, brdd (5.8, 14.0)	1.96, m	1.72, dd (9.5, 14.1)
		2.13, m	2.12, m		2.26, dd (6.0, 14.6)
14	2.27, m	2.25, m	2.24, brd (21.4)	2.26, brd (19.1)	3.25, m
	2.62, m	2.79, m	2.81, m	2.60, m	
15	5.94, brd (9.9)	5.95, brd (10.9)	5.95, brd (9.9)	5.94, brd (9.9)	6.16, d (10.2)
16	5.63, m	5.54, brd (10.9)	5.50, dq (2.0, 9.9)	5.51, m	5.56, ddd (2.2, 4.7, 5.5)
17	2.76, br t (5.8)	3.23, br m	3.19, br m	2.80, br t (6.5)	2.80, dd (5.5, 9.0)
18	5.65, dd (15.5, 7.2)	5.82, ddd (1.5, 8.8, 15.4)	5.66, dd (7.7, 15.4)	5.65, dd (7.7, 15.6)	5.65, dt (9.7, 16.9)
19	5.64, m	5.76, dd (3.9, 15.4)	5.67, dd (5.8, 15.4)	5.57, dd (5.9, 15.6)	5.27, d (10.0)
					5.21, d (16.9)
20	4.16, t (4.8)	4.19, m	4.16, m	4.20, t (5.3)	3.22, dd (3.1, 9.7)
21	4.30, m	4.27, m	4.16, m	4.07, quad (6.9)	4.28, d (5.0)
22	1.55, m	1.59, m	1.60, m	1.59, m	1.53, dd (1.2, 5.9, 13.7)
	2.39, m	2.39, m	2.39, q (6.5)	2.40, dt (6.6, 12.6)	2.39, ddd (6.6, 8.2, 14.0)
23	3.94, sext (6.3)	4.07, m	4.22, m	4.26, sext (7.4)	3.96, m
24	1.34, d (6.2)	1.34, d (6.1)	1.32, d (6.3)	1.32, d (6.2)	1.34, d (6.2)

Compound **5** has a terminal methylene group (at δ_C 119.6, δ_H 5.27 and δ_H 5.21) while the tetrahydrofuran moiety connected to C-19 in **1** is connected to C-14 in **5**.

Based on COSY correlations (**Figure 5**), the sporothriolide moiety was the same in compound **5** as in **1**. Moreover, COSY correlations from H-13 to H-19 through H-14 (δ_H 3.25), H-15 (δ_H 6.16), H-16 (δ_H 5.56), H-17 (δ_H 2.80) and H-18 (δ_H 5.65) together with HMBC correlation between H-13 and C-3 and H-17 and C-3 formed a cyclohexane fragment like in **1**. Finally, by using the COSY correlations from H-24 (δ_H 1.34) to H-20 (δ_H 3.22), through H-23 (δ_H 3.96), H-22 (δ_H 1.53 and 2.39) and H-21 (δ_H 4.28) we deduce the tetrahydrofuran moiety. The HMBC correlations between H-20 and C-14 and C-15 allowed us to connect this tetrahydrofurane moiety to the sp^3 methine C-14.

The absolute configuration of sporochartine E (**5**) was suggested using ROE correlations compared to the absolute configuration of sporochartine A (**1**) (**Figure 6**).

ROE correlations between H-2 and H-5/H-6 in the sporothriolide moiety and the ROE correlation between H-20 and H-21 and between H-23 and H-21 in the tetrahydrofuran moiety indicated a similar to that in **1**.

Sporochartine E (**5**), showed a correlation between H-17 and H-2, like in compounds **1** and **4**. H-2 also exhibited a correlation with H-13b but not with H-14. This suggests that C-3 and C-17 has the same relative configuration than **4**. For C-14, we observed ROE correlations between H-14 and H-13a, H-13a, and H-17 and H-14 and H-24, suggesting a *3R, 14S, 17S* configuration for compound **5**.

Based on the structure of sporothriolide and the recently reported trienylfuranol A isolated from *H. submoniticulosum*, we suggested a hypothetic biosynthetic pathway of sporochartines, involving a "spiro" Diels-Alderase reaction as shown in **Figure 7** (Klas et al., 2015; Byrne et al., 2016). The possibility of a non-enzymatic catalysis was excluded as reported previously (Leman-Loubière et al., 2017).

The cytotxicity of sporochartines was evaluated on three human cancer cell lines, HCT-116 (human colon carcinoma), PC-3 (**prostate cancer cell lines)** and MCF-7 (breast **cancer cell** line). The results presented in **Table 3** are highly contrasting but nevertheless clearly indicate the impact of sporochartine conformation on the bioassay results.

Thus, sporochartine C (**3**) is toxic against the three cell lines with IC_{50} ranging from 7.2 to 21.5 μM. In contast, sporochartine A (**1**) is totally inactive at concentrations higher than 100 μM. This may be due to the substantial difference in the spatial conformation of compounds **1** and **3** (**Figure 4**).

TABLE 2 | ^{13}C NMR data for sporochartines A–E (Data acquired in $CDCl_3$ at 125 MHz).

Position	Sporochartine A	Sporochartine B	Sporochartine C	Sporochartine D	Sporochartine E
	δ_C	δ_C	δ_C	δ_C	δ_C
1	171.8, C	173.1, C	172.8, C	171.9, C	172.7, C
2	50.6, CH	47.2, CH	47.2, CH	50.9, CH	49.7, CH
3	51.0, C	51.0, C	50.9, C	49.2, C	46.3, C
4	177.0, C	178.7, C	178.6, C	176.2, C	175.6, C
5	78.2, CH	78.7, CH	78.7, CH	78.0, CH	76.4, CH
6	81.2 CH	81.7 CH	81.1 CH	81.3 CH	81.6, CH
7	28.9, CH_2	28.9, CH_2	29.0, CH_2	29.0, CH_2	29.0, CH_2
8	25.5, CH_2	25.3, CH_2	25.6, CH_2	25.5 CH_2	25.5, CH_2
9	29.1, CH_2	29.1, CH_2	29.1, CH_2	29.2, CH_2	29.1, CH_2
10	31.7, CH_2	31.7, CH_2	31.7, CH_2	31.8, CH_2	31.7, CH_2
11	22.7, CH_2	22.9, CH_2	22.9, CH_2	22.7, CH_2	22.7, CH_2
12	14.2, CH_3	14.3, CH_3	14.2, CH_3	14.3, CH_3	14.2, CH_3
13	20.9, CH_2	26.9, CH_2	27.1, CH_2	20.9, CH_2	24.1, CH_2
14	22.7, CH_2	22.7, CH_2	22.7, CH_2	22.6, CH_2	32.6, CH
15	129.4, CH	130.0, CH	130.2, CH	129.8, CH	130.9, CH
16	124.0, CH	124.8, CH	124.6, CH	123.5 CH	124.1, CH
17	45.5, CH	47.0, CH	46.5, CH	43.9, CH	46.9, CH
18	131.6, CH	130.9, CH	130.6, CH	129.1, CH	136.8, CH
19	131.5, CH	130.1, CH	134.3, CH	134.1, CH	119.6, CH_2
20	83.3, CH	82.8, CH	84.8, CH	84.9, CH	87.0, CH
21	74.8, CH	73.9, CH	77.3, CH	77.1, CH	72.5, CH
22	42.6, CH_2	42.4, CH_2	42.3, CH_2	41.2, CH_2	43.4, CH_2
23	74.3, CH	74.2, CH	74.1, CH	74.1, CH	73.9, CH
24	21.7 CH_3	22.5 CH_3	22.4 CH_3	22.5 CH_3	22.6, CH_3
$[\alpha]_D^{25}$	−57° (0.5, $CHCl_3$)	+72° (1.0, $CHCl_3$)	+93° (0.27, $CHCl_3$)	−152° (0.27, $CHCl_3$)	+51° (*c* 0.3, $CHCl_3$)
$[M+H]^+$ HRESIMS	419.2423	419.2423	419.2431	419.2429	419.2433
IR	3,521, 2,929, 2,859, 1,771, 1,452, 1,304, 1,175, 1,019 cm^{-1}	3,468, 2,934, 2,863, 1,770, 1,303, 1,179, 1,071 cm^{-1}	3,441, 2,957, 2,928, 2,858, 1,770, 1,454, 1,177, 1,017 cm^{-1}	3,435, 2,932, 1,771, 1,178, 1,019 cm^{-1}	3,501, 2,931, 1,766, 1,308, 1,187, 1,075 cm^{-1}

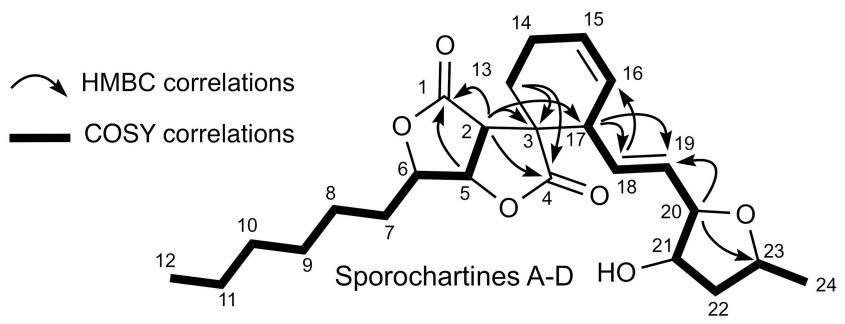

FIGURE 3 | COSY and HMBC key connectivities for sporochartines A–D.

The lower IC_{50} values were recorded for different sporochartines and against different cell lines, sporochartine B (**2**) for MCF-7 (2.28 μM), sporochartine C (**3**) for HCT-116 (7.2 μM) and sporochartine E (**5**) for PC-3 (5.96 μM).

Our future efforts will focus on the cytotoxic profile, biosynthesis and synthesis of sporochartines. The cytotoxicity profile reveals a non-cytotoxic sporochartine A (**1**), a large spectrum cytotoxic sporochartine C (**3**) and more cell line specific

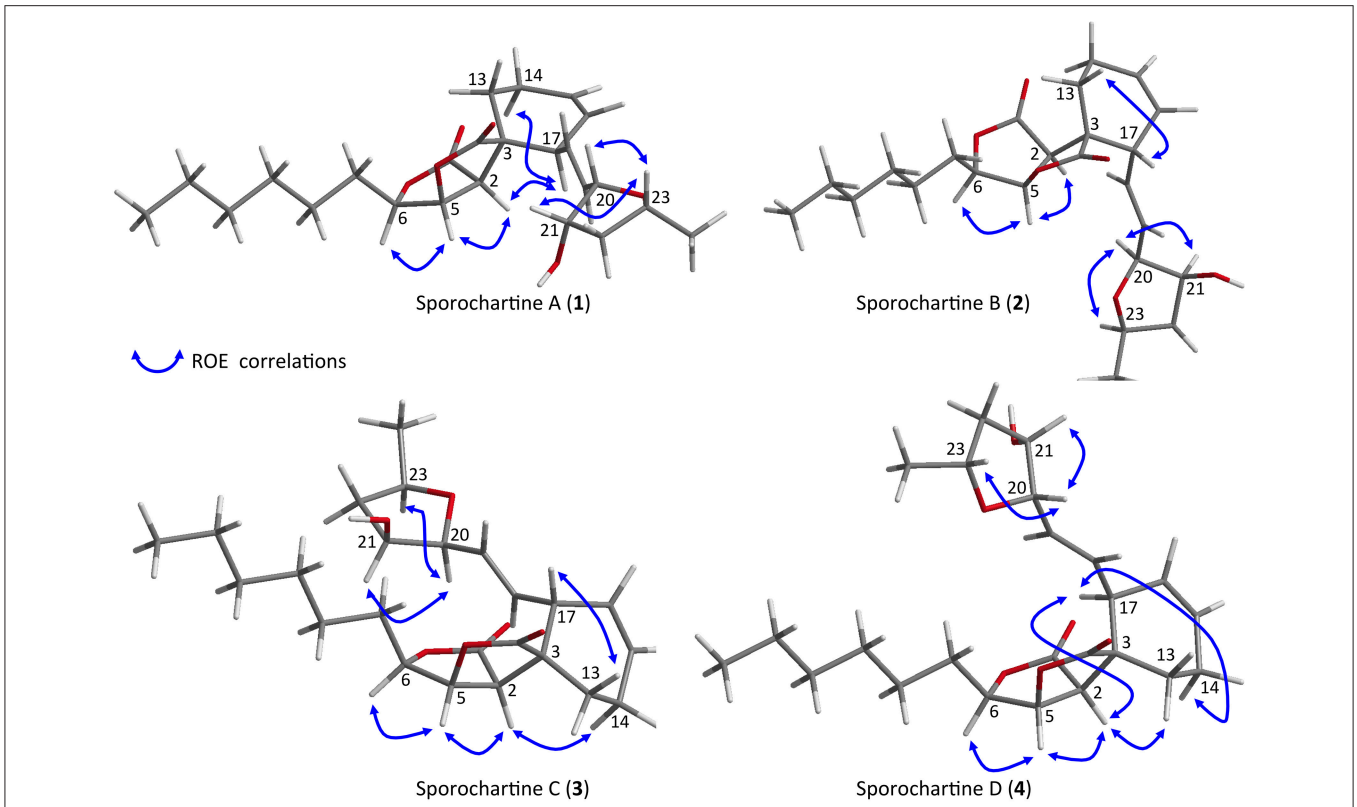

FIGURE 4 | Key ROE correlations for sporochartines A–D reported on Chem-3D figures.

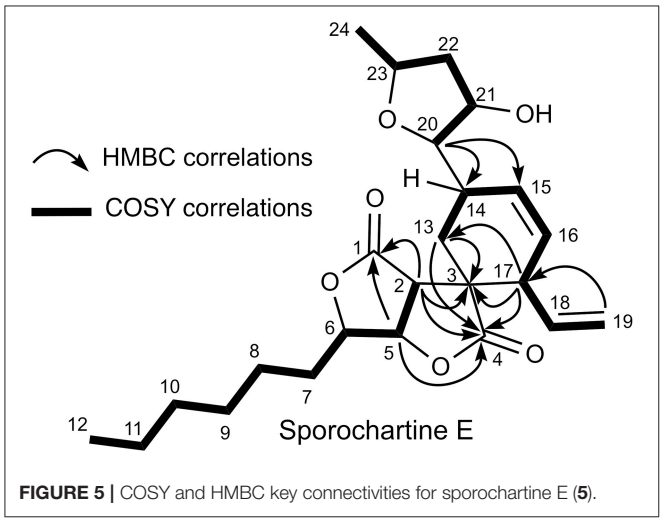

FIGURE 5 | COSY and HMBC key connectivities for sporochartine E (**5**).

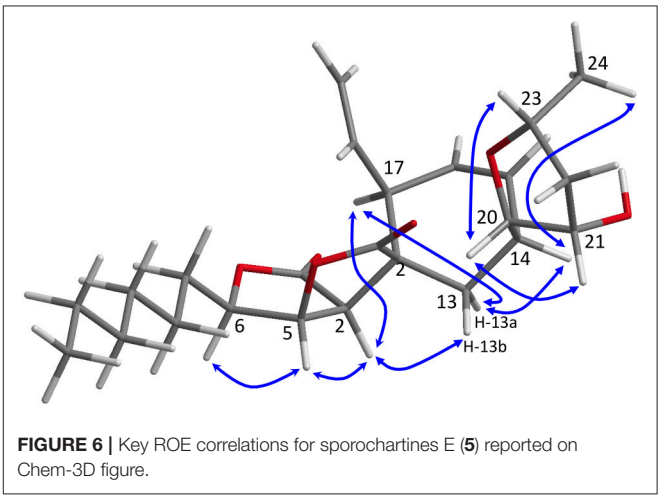

FIGURE 6 | Key ROE correlations for sporochartines E (**5**) reported on Chem-3D figure.

sporochartines B (**2**), D (**4**), and E (**5**). This finding merits future investigation on the mechanisms of action of these new scaffolds of cytotoxic compounds.

The biosynthesis of sporochartines, and the biosynthesis of its two moieties, sporothriolide and trienylfuranol A are still unknown. This opens new and promising opportunities for the discovery of novel biosynthetic microbial clusters.

Finally, having in hand hundreds of milligrams of sporothriolide, the hemi-synthesis of sporochartines is currently in progress based on a final Diels-Alder connection. The selectivity of the chemical catalysis and the proportion of different isomers will be compared to the microbial counterpart. According to our expertise in biocatalysis-based chemodiversification of natural compounds (Adelin et al., 2011; Martins et al., 2015), sporothriolide will be submitted to a

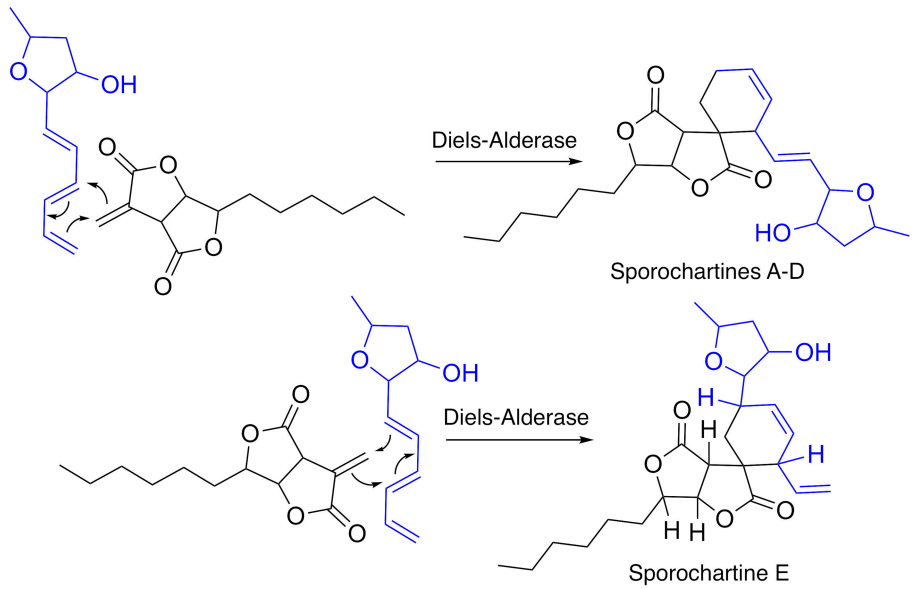

FIGURE 7 | Hypothetic biosynthesis of sporochartines through Diels-Alderase type reaction between sporothriolide and trienylfuranol A.

TABLE 3 | IC_{50} values recorded for sporochartines A–E against three cancer cell lines, HCT-116 (human colon carcinoma), PC-3 (human prostate cancer cell lines), and MCF-7 (human breast cancer cell line).

	IC_{50} in μM		
	HCT116	**PC3**	**MCF7**
Sporochartine A (**1**)	>100	>100	>100
Sporochartine B (**2**)	28.7 ± 2.5	>100	2.28 ± 0.1
Sporochartine C (**3**)	7.2 ± 0.21	13.4 ± 1.2	21.5 ± 0.3
Sporochartine D (**4**)	>100	15.2 ± 1.7	>100
Sporochartine E (**5**)	>100	5.96 ± 0.28	>100

panel of microorganisms in order to pursue the enrichment of sporothriolide related compounds.

MATERIALS AND METHODS

General Experimental Procedures

Optical rotations $[\alpha]_D$ were measured using an Anton Paar MCP-300 polarimeter. IR spectra were obtained using a Perkin Elmer BX FT-IR spectrometer. NMR experiments were performed using a Bruker Avance 500 MHz in $CDCl_3$ at room temperature. High-resolution mass spectra were obtained on a Waters LCT Premier XE spectrometer equipped with an ESI-TOF (electrospray-time of flight) by direct infusion of the purified compounds. Preparative HPLC was performed using Waters modules consisting of an autosampler 717, a pump 600, a photodiode array detector 2996 and an evaporative light-scattering detector, ELSD 2420. Prepacked silica gel Redisep columns were used for flash chromatography using a Combiflash-Companion chromatogram (Serlabo, France). All other chemicals and solvents were purchased from SDS (France).

Animal Material

The *Sphaerocladina* sponge was collected on 17 December 2015 from the coast of Tahiti (9°45.421′S–139°08.275′W) at 20 m depth (Leman-Loubière et al., 2017).

Hypoxylon Identification and Cultivation

H. monticulosum CLL205 was isolated from the sponge *Sphaerocladina* and grown at 28°C on a PDB medium (Potatoes Dextrose Broth, DIFCO). The ITS rDNA gene amplification and sequencing were performed, and submitted to NCBI/BLAST database (GenBank). The primers used for PCR amplification were ITS1 F: CTT GGT CAT TTA GAG GAA GTA A (T_m: 55°C) and ITS4: TCC TCC GCT TAT TGA TATGC (T_m: 53°C). The GenBank accession number for *H. monticulosum* CLL205 sequence is SUB2477083 25758633.seq KY744359. *H. monticulosum* CLL205 was cultivated in a 2 L Erlenmeyer containing 1L of PDB medium (DIFCO) in a rotary shaker at 28°C and 130 rpm.

Compounds Isolation

The culture broth was extracted with ethyl acetate (3×500 mL). The solvent was concentrated to dryness *in vacuo* to afford 430 mg of crude extract. 300 mg were submitted to flash chromatography on a Combiflash Companion using a Redisep 12 g silica column, eluted with a heptane-ethyl acetate mixture. After concentration *in vacuo*, we obtained sporothriolide (30 mg), compound **1** (9 mg), **2** (14 mg), **3** (4 mg), **4** (3 mg), **5** (1 mg).

Cytotoxicity Assays

A tetrazolium dye [3-(4,5-dimethylthiazol-2-yl)-2,5-diphenyltetrazolium-bromide; MTT]-based colorimetric assay was used to measure the inhibition on the proliferation of various human tumor cell lines HCT-116 (human colon carcinoma), PC-3 (**prostate cancer cell lines)** and MCF-7 (breast **cancer cell** line). The tested compounds were formulated in DMSO and added to the cells such that the final DMSO concentration ranged from 1 to 3%. Cells were grown in D-MEM medium supplemented with 10% fetal calf serum (Invitrogen), in the presence of penicillin, streptomycin, and fungizone, and plated in 96-well microplates. After 24 h of growth, cells were treated with target compounds from 100 μM to 10 nM. After 72 h, MTS reagent (Promega) was added, and the absorbance was monitored (490 nm) to measure the inhibition of cell proliferation compared to untreated cells. IC_{50} determination experiments were performed in separate duplicate experiments.

Isolated Compounds

Sporochartine A (**1**)[33]: white needles, M.p. 86.5–87.9°C; $[\alpha]_D^{25}$ −57 (*c* 0.5, $CHCl_3$). See **Tables 1**, **2** for complete ^1H, ^{13}C NMR and IR data. HRESIMS *m/z* 419.2433 $[M + H]^+$ (calcd for $C_{24}H_{35}O_6$, 419.2433).

Sporochartine B (**2**): white powder; $[\alpha]_D^{25}$ +72 (*c* 1.0, $CHCl_3$). See **Tables 1**, **2** for complete ^1H, ^{13}C NMR and IR data. HRESIMS *m/z* 419.2419 $[M + H]^+$ (calcd for $C_{24}H_{35}O_6$, 419.2433).

Sporochartine C (**3**): white powder (4 mg); $[\alpha]_D^{25}$ +93 (*c* 0.27, $CHCl_3$). See **Tables 1**, **2** for complete ^1H, ^{13}C NMR and IR data. HRESIMS *m/z* 419.2433 $[M + H]^+$ (calcd for $C_{24}H_{35}O_6$, 419.2433).

Sporochartine D (**4**): white powder; $[\alpha]_D^{25}$ −152 (*c* 0.27, $CHCl_3$). See **Tables 1**, **2** for complete ^1H, ^{13}C NMR and IR data. HRESIMS *m/z* 419.2431 $[M + H]^+$ (calcd for $C_{24}H_{35}O_6$, 419.2433).

Sporochartine E (**5**): white powder; $[\alpha]_D^{25}$ +51 (*c* 0.3, $CHCl_3$). See **Tables 1**, **2** for complete ^1H, ^{13}C NMR and IR data. HRESIMS *m/z* 419.2425 $[M + H]^+$ (calcd for $C_{24}H_{35}O_6$, 419.2434).

Structural elucidation data are reported in the Supplementary Materials.

ASSOCIATED CONTENT

Detailed 1D and 2DNMR, MS and IR spectra of sporochartines are available free of charge via the Internet at http://pubs.acs.org.

AUTHOR CONTRIBUTIONS

CL-L: microbiologie chemistry; GL: chemistry; CD: invetebrate investigation; JO: head of the team and science manager.

ACKNOWLEDGMENTS

This work was supported by TASCMAR project funded by the European Union's Horizon 2020 research and innovation program under grant agreement n° 634674, and the Ph.D. support program of ICSN.

The authors are grateful to the CIBI Plateforme of CNRS-ICSN for cytotoxicity essays (Jérôme Bignon & Hélène Levaique).

SUPPLEMENTARY MATERIAL

The Supplementary Material for this article can be found online at: https://www.frontiersin.org/articles/10.3389/fmars.2017.00399/full#supplementary-material

REFERENCES

Adelin, E., Servy, C., Cortial, S., Lévaique, H., Gallard, J.-F., Martin, M.-T., et al. (2011). Biotransformation of natural compounds. Oxido-reduction of Sch-642305 by *Aspergillus ochraceus* ATCC 1009. *Bioorg. Med. Chem. Lett.* 21, 2456–2459. doi: 10.1016/j.bmcl.2011.02.063

Angawi, R. F., Swenson, D. C., Gloer, J. B., and Wicklow, D. T. (2005). Malettinins B–D: new polyketide metabolites from an unidentified fungal colonist of hypoxylon stromata (NRRL 29110). *J. Nat. Prod.* 68, 212–216. doi: 10.1021/np049625r

Bills, G. F., González-Menéndez, V., Martin, J., Platas, G., and Fournier, J. (2012). *Hypoxylon pulicicidum* sp. nov. (Ascomycota, Xylariales), a pantropical insecticide-producing endophyte. *PLoS ONE* 7:e46687. doi: 10.1371/journal.pone.0046687

Bodo, B. D., Davoust, D., Lecommandeur, D., Rebuffat, S., Genetet, I., and Pinon, J. (1987). Hymatoxin A, a diterpene sulfate phytotoxin of *Hypoxylon mammatum*, parasite of aspen. *Tetrahedron Lett.* 28, 2355–2358. doi: 10.1016/S0040-4039(00)96123-9

Borgschulte, K., Rebuffat, S., Trowitzsch-Kienast, W., Schomburg, D., Pinon, J., and Bodo, B. (1991). Isolation and structure elucidation of hymatoxins B–E and other phytotoxins from *Hypoxylon mammatum* fungal pathogen of leuce poplars. *Tetrahedron* 47, 8351–8360. doi: 10.1016/S0040-4020(01)96176-9

Burgess, K. M. N., Ashraf Ibrahim, A., Sørensen, D., and Sumarah, M. W. (2017). Trienylfuranol A and trienylfuranone A-B: metabolites isolated from an endophytic fungus, *Hypoxylon submoniticulosum*, in the raspberry *Rubus idaeus*. *J. Antibiot.* 70, 721–725. doi: 10.1038/ja.2017.18

Byrne, M. J., Lees, N. R., Han, L.-C., Van der Kamp, M. W., Mulholland, A. J., Stach, J. E. M., et al. (2016). The catalytic mechanism of a natural diels–alderase revealed in molecular detail. *J. Am. Chem. Soc.* 138, 6095–6098. doi: 10.1021/jacs.6b00232

Cao, L.-L., Zhang, Y.-Y., Liu, Y.-J., Yang, T.-T., Zhang, J.-L., Zhang, Z.-G., et al. (2016). Anti-phytopathogenic activity of sporothriolide, a metabolite from endophyte *Nodulisporium* sp. A21 in *Ginkgo biloba*. *Pestic. Biochem. Physiol.* 129, 7–13. doi: 10.1016/j.pestbp.2015.10.002

Daferner, M., Mensch, S., Anke, T., and Sternerb, O. (1999). Hypoxysordarin, a New Sordarin Derivative from Hypoxylon croceum. *Z. Naturforsch.* 54c, 474–480. doi: 10.1515/znc-1999-7-803

Espada, A., Rivera-Sagredo, A., De la Fuente, J. M., Hueso-Rodriguez, J. A., and Elson, S. W. (1997). New cytochalasins from the fungus *Xylaria hypoxylon*. *Tetrahedron* 53, 6485–6492. doi: 10.1016/S0040-4020(97)00305-0

Fernandes, R. A., and Ingle, A. B. (2009). Chiral vicinal diols as platforms for separable diastereomers in Johnson–Claisen rearrangement: a new short route to (–)-nor-canadensolide, (–)-canadensolide and (–)-sporothriolide. *Tetrahedron Lett.* 50, 1122–1124. doi: 10.1016/j.tetlet.2008.12.084

Fukai, M., Tsukada, M., Miki, K., Suzuki, T., Sugita, T., Kinoshita, K., et al. (2012). Hypoxylonols C–F, Benzo[j]fluoranthenes from Hypoxylon truncatum. *J. Nat. Prod.* 75, 22–25. doi: 10.1021/np2004193

Gu, W., Ge, H. M., Song, Y. C., Ding, H., Zhu, H. L., Zhao, X. A., et al. (2007). Cytotoxic Benzo[j]fluoranthene metabolites from Hypoxylon truncatum IFB-18, an endophyte of *Artemisia annua*. *J. Nat. Prod.* 70, 114–117. doi: 10.1021/np0604127

Ishihara, J., Tsuru, H., and Hatakeyama, S. (2014). Total synthesis of (–)-dihydrosporothriolide utilizing an indium-mediated reformatsky–claisen rearrangement. *J. Org. Chem*. 79, 5908–5913. doi: 10.1021/jo5008948

Klas, K., Tsukamoto, S., Sherman, D. H., and Williams, R. M. (2015). Natural diels–alderases: elusive and irresistable. *J. Org. Chem*. 80, 11672–11685. doi: 10.1021/acs.joc.5b01951

Krohn, K., Ludewig, K., Aust, H.-J., Draeger, S., and Schulz, B. (1994). Biologically active metabolites from fungi. 3. sporothriolide, discosiolide, and 4-epi-ethisolide–new furofurandiones from *Sporothrix* sp., *Discosia* sp., and *Pezicula livida*. *J. Antibiot.* 47, 113–118. doi: 10.7164/antibiotics.47.113

Kuhnert, E., Heitkämper, S., Fournier, J., Surup, F., and Stadler, M. (2014). Hypoxyvermelhotins A–C, new pigments from *Hypoxylon lechatii* sp. nov. *Fungal Biol*. 118, 242–252. doi: 10.1016/j.funbio.2013.12.003

Kuhnert, E., Surup, F., Herrmann, J., Huch, V., Müller, R., and Stadler, M. (2015a). Rickenyls A–E, antioxidative terphenyls from the fungus *Hypoxylon rickii* (Xylariaceae, Ascomycota). *Phytochemistry* 118, 68–73. doi: 10.1016/j.phytochem.2015.08.004

Kuhnert, E., Surup, F., Sir, E. B., Lambert, C., Hyde, K. D., Hladki, A. I., et al. (2015b). Lenormandins A–G, new azaphilones from *Hypoxylon lenormandii* and *Hypoxylon jaklitschii* sp. nov., recognised by chemotaxonomic data. *Fungal Divers*. 71, 165–184. doi: 10.1007/s13225-014-0318-1

Kuhnert, E., Surup, F., Wiebach, V., Bernecker, S., and Stadler, M. (2015c). Botryane, noreudesmane and abietane terpenoids from the ascomycete *Hypoxylon rickii*. *Phytochemistry* 117, 116–122. doi: 10.1016/j.phytochem.2015.06.002

Leman-Loubière, C., Le Goff, G., Retailleau, P., Debitus, C., and Ouazzani, J. (2017). Sporothriolide-related compounds from the fungus *Hypoxylon monticulosum* CLL-205 isolated from a sphaerocladina sponge from the tahiti coast. *J. Nat. Prod.* 80, 2850–2854. doi: 10.1021/acs.jnatprod.7b00714

Linh, D. T. P., Hien, B. T. T., Que, D. D., Lam, D. M., Arnold, N., Schmidt, J., et al. (2014). Cytotoxic constituents from the vietnamese fungus xylaria schweinitzii. *Nat. Prod. Commun*. 9, 659–660.

Martins, M. P., Ouazzani, J., Arcile, G., Jeller, A. H., de Lima, J. P. F., Seleghim, M. H. R., et al. (2015). Biohydroxylation of (–)-Ambrox®, (–)-Sclareol, and (+)-Sclareolide by whole cells of Brazilian marine-derived fungi. *Mar. Biotechnol*. 17, 211–218. doi: 10.1007/s10126-015-9610-7

Quang, D. N., Hashimoto, T., Nomura, Y., Wollweber, H., Hellwig, V., Fournier, J., et al. (2005a). Cohaerins A and B, azaphilones from the fungus Hypoxylon cohaerens, and comparison of HPLC-based metabolite profiles in *Hypoxylon* sect. *Annulata*. *Phytochemistry* 66, 797–809. doi: 10.1016/j.phytochem.2005.02.006

Quang, D. N., Hashimoto, T., Stadler, M., and Asakawa, Y. (2005b). Dimeric azaphilones from the xylariaceous ascomycete *Hypoxylon rutilum*. *Tetrahedron* 61, 8451–8455. doi: 10.1016/j.tet.2005.06.077

Quang, D. N., Hashimoto, T., Tanaka, M., Stadler, M., and Asakawa, Y. (2004). Cyclic azaphilones daldinins E and F from the ascomycete fungus *Hypoxylon fuscum* (Xylariaceae). *Phytochemistry* 65, 469–473. doi: 10.1016/j.phytochem.2003.09.022

Quang, D. N., Stadler, M., Fournier, J., and Asakawa, Y. (2006). Carneic Acids A and B, chemotaxonomically significant antimicrobial agents from the xylariaceous ascomycete *Hypoxylon carneum*. *J. Nat. Prod*. 69, 1198–1202. doi: 10.1021/np0602057

Sánchez-Ballesteros, J., González, V., Salazar, O., Acero, J., Portal, M. A., Julián, M., et al. (2000). Phylogenetic study of Hypoxylon and related genera based on ribosomal ITS sequences. *Mycologia* 92, 964–977. doi: 10.2307/3761591

Schlingmann, G., Milne, L., and Carter, G. T. (2002). Isolation and identification of antifungal polyesters from the marine fungus *Hypoxylon oceanicum* LL-15G256. *Tetrahedron* 58, 6825–6835. doi: 10.1016/S0040-4020(02)00746-9

Sharma, G. V. M., and Krishnnudu, K. (1995). Radical reactions on furanoside acetals: first synthesis of sporothriolide and 4-epi- ethisolide from 'diacetone glucose'. *Tetrahedron Lett.* 36, 2661–2664. doi: 10.1016/0040-4039(95)00327-9

Stadler, M., Fournier, J., Laessøe, T., Lechat, C., Tichy, H., and Piepenbring, M. (2008). Recognition of hypoxyloid and xylarioid Entonaema species and allied Xylaria species from a comparison of holomorphic morphology, HPLC profiles, and ribosomal DNA sequences. *Mycol. Prog.* 7, 53–73. doi: 10.1007/s11557-008-0553-5

Stadler, M., Quang, D. N., Tomita, A., Hashimoto, T., and Asakawa, Y. (2006). Changes in secondary metabolism during stromatal ontogeny of Hypoxylon fragiforme. *Mycol. Res.* 110, 811–820. doi: 10.1016/j.mycres.2006.03.013

Sudarman, E., Kuhnert, E., Hyde, K. D., Sir, E. B., Surup, F., and Marc Stadler, M. (2016). Truncatones A–D, benzo[j]fluoranthenes from Annulohypoxylon species (Xylariaceae, Ascomycota). *Tetrahedron* 72, 6450–6454. doi: 10.1016/j.tet.2016.08.054

Surup, F., Kuhnert, E., Lehmann, E., Heitkämper, S., Hyde, K. D., Fournier, J., et al. (2014). Sporothriolide derivatives as chemotaxonomic markers for *Hypoxylon monticulosum*. *Mycology* 5, 110–119. doi: 10.1080/21501203.2014.929600

Surup, F., Mohr, K. I., Jansen, R., and Stadler,. M. (2013). Cohaerins G–K, azaphilone pigments from Annulohypoxylon cohaerens and absolute stereochemistry of cohaerins C–K. *Phytochemistry* 95, 252–258. doi: 10.1016/j.phytochem.2013.07.027

Yu, M., Lynch, V., and Pagenkopf, B. L. (2001). Intramolecular cyclopropanation of glycals: studies toward the synthesis of canadensolide, sporothriolide, and xylobovide. *Org. Lett.* 3, 2563–2566. doi: 10.1021/ol016239h

Conflict of Interest Statement: The authors declare that the research was conducted in the absence of any commercial or financial relationships that could be construed as a potential conflict of interest.